RESEARCH ARTICLE | NOVEMBER 18 2024

Perturbative analysis of the coherent state transformation in *ab initio* cavity quantum electrodynamics

Peyton Roden ; Jonathan J. Foley, IV

J. Chem. Phys. 161, 194103 (2024)
https://doi.org/10.1063/5.0233717

The Journal of Chemical Physics ARTICLE pubs.aip.org/aip/jcp

Perturbative analysis of the coherent state transformation in *ab initio* cavity quantum electrodynamics

Cite as: J. Chem. Phys. 161, 194103 (2024); doi: 10.1063/5.0233717
Submitted: 16 August 2024 • Accepted: 28 October 2024 •
Published Online: 18 November 2024

Peyton Roden and Jonathan J. Foley IV[a)]

AFFILIATIONS

Department of Chemistry, University of North Carolina Charlotte, 9201 University City Boulevard, Charlotte, North Carolina 28223, USA

[a)]**Author to whom correspondence should be addressed:** jfoley19@charlotte.edu

ABSTRACT

Experimental demonstrations of modified chemical structure and reactivity under strong light–matter coupling have spurred theoretical and computational efforts to uncover underlying mechanisms. *Ab initio* cavity quantum electrodynamics (QED) combines quantum chemistry with cavity QED to investigate these phenomena in detail. Unitary transformations of *ab initio* cavity QED Hamiltonians have been used to make them more computationally tractable. We analyze one such transformation, the coherent state transformation, using perturbation theory. Applying perturbation theory up to third order for ground state energies and potential energy surfaces of several molecular systems under electronic strong coupling, we show that the coherent state transformation yields better agreement with exact ground state energies. We examine one specific case using perturbation theory up to ninth order and find that coherent state transformation performs better up to fifth order but converges more slowly to the exact ground state energy at higher orders. In addition, we apply perturbation theory up to second order for cavity mode states under bilinear coupling, elucidating how the coherent state transformation accelerates the convergence of the photonic subspace toward the complete basis limit and renders molecular ion energies origin invariant. These findings contribute valuable insights into computational advantages of the coherent state transformation in the context of *ab initio* cavity quantum electrodynamics methods.

I. INTRODUCTION

Strong interactions between photons resonant with molecular transitions can lead to the emergence of new hybrid light–matter states, known as polariton states, which can effect dramatic changes in chemical structure and reactivity.[1–20] The emerging field of polariton chemistry seeks to understand and leverage these changes in chemical structure and dynamics to perform novel chemistry, and computational modeling has played a key role in shaping this understanding. For one or a few molecules under electronic strong coupling, cavity quantum electrodynamics provides the tools to treat the photonic degrees of freedom, and *ab initio* quantum chemistry provides the tools to treat the electronic degrees of freedom. The marriage of these approaches is often referred to as *ab initio* cavity quantum electrodynamics (ai-QED), which has seen a surge of developments in recent years.[18,21–51] Traditional quantum chemistry already presents a challenging example of the many-body problem, and strong coupling to photons introduces additional difficulties that must be overcome to yield accurate and computationally facile approaches.

Unitary transformations have a long history in the development of many-body theories, where a common strategy is to identify or design transformations that bring a many-body Hamiltonian into a representation, which is more computationally tractable.[52–56] Recent efforts to develop computationally tractable and predictive methods for molecules under strong light–matter coupling has brought these techniques to bear on ai-QED Hamiltonians to partially decouple the light–matter interactions that arise in this context.[43,57–60] In the Pauli–Fierz Hamiltonian that is the basis for much of the work on ai-QED, there are several examples of unitary transformations that are based upon products of the photonic momentum operator and the matter dipole operator (which is the matter position operator

scaled by the electron charge). These transformations impart shifts in the photonic positions and the matter momenta and render the Pauli–Fierz Hamiltonian diagonal in the infinite coupling limit. In particular, Koch and co-workers,[59] as well as Li and Zhang,[60] have used such unitary transformations to parameterize reference states for QED Hartree–Fock procedures that have many attractive properties at arbitrary coupling strengths, including energies and orbitals that are fully origin invariant. Reichman and co-workers[43] recently investigated an analogous approach for correlated theories where, similar to the approach of Zhang and Li for QED Hartree–Fock, the transformation is variationally optimized, yielding the so-called Lang–Firsov transformation. In the current work, we focus on a related but simpler unitary transformation known as the coherent state transformation, which shares a similar form as the transformations discussed in the independent investigations in Refs. 43, 59, and 60 with a key difference being that it is formulated as a product of the photonic momentum operator with the *expectation value* of the matter dipole operator. The coherent state transformation thus shifts the photonic coordinates but does not transform the matter degrees of freedom. The coherent state transformation has been used to parameterize QED Hartree–Fock reference wavefunctions[29,36] and in correlated ai-QED calculations,[37,41,48,61] has been shown to yield origin invariant energies (not orbitals), and can significantly accelerate the convergence of the photonic subspace. In this work, we utilize perturbation theory to elucidate how the coherent state transformation engenders these favorable properties in ai-QED calculations. We specifically formulate perturbation theory using the Pauli–Fierz Hamiltonian and its coherent state transformed analog projected onto a tensor product basis of photonic Fock states and adiabatic many-electron states from cavity-free electronic structure calculations. In other words, we use a parameterized ai-QED approach that avoids the need to make any modifications to the underlying quantum chemistry method. We find that applying the coherent state transformation yields second- and third-order estimates to the ground state energy that are in consistently better agreement with the exact ground state across a range of coupling strengths compared to the same orders without transformation of the Hamiltonian. We apply arbitrary order perturbation theory for one test system to confirm that perturbative series for both the Pauli–Fierz Hamiltonian and its coherent state transformed analog converge to the exact answer. Surprisingly, in this test case, we find that the advantage of the coherent state transformation is only a feature of low orders of correction and that perturbative corrections of order 6 and higher to the Pauli–Fierz Hamiltonian yield better agreement with the exact ground state. We hypothesize that this behavior is consistent with the coherent state transformation primarily enhancing the convergence with respect to the photonic subspace. To further elucidate this feature, we treat the bilinear coupling between matter and photon degrees of freedom as a perturbation to the cavity Hamiltonian, which reveals that the coherent state transformation decouples the photonic subsystem from the matter subsystem to within a magnitude that is related to the error in the reference estimate of the dipole moment expectation value that parameterizes the transformation for a target coupled state. Importantly, this error is manifestly origin invariant, and so this result sheds light on why the coherent state transformation accelerates photon convergence and restores origin invariance in ai-QED calculations.

II. THEORY

The starting point for many ai-QED treatments of molecular polariton systems is the Pauli–Fierz Hamiltonian in the dipole approximation,[62] which we write in atomic units as

$$\hat{H}_{\mathrm{PF}} = \hat{H}_e + \omega\left(\hat{b}^\dagger\hat{b} + \frac{1}{2}\right) - \sqrt{\frac{\omega}{2}}\hat{d}(\hat{b}^\dagger + \hat{b}) + \frac{1}{2}\hat{d}^2. \tag{1}$$

In Eq. (1), $\hat{H}_e$ is the standard electronic Hamiltonian within the Born–Oppenheimer approximation,[63] and $\hat{H}_{\mathrm{cav}} = \omega\left(\hat{b}^\dagger\hat{b} + \frac{1}{2}\right)$ is the bare Hamiltonian for the cavity photon mode, where ω represents the frequency and $\hat{b}^\dagger$ and $\hat{b}$ are raising and lowering operators for the photon mode, respectively. The last two terms capture the coupling between the photonic and matter degrees of freedom and are called the bilinear coupling, $\hat{H}_{\mathrm{blc}} = -\sqrt{\frac{\omega}{2}}\,\hat{d}\,(\hat{b}^\dagger + \hat{b})$, and dipole self-energy terms $\hat{H}_{\mathrm{dse}} = \frac{1}{2}\hat{d}^2$, respectively. In these interaction terms, $\hat{d} = \boldsymbol{\lambda}\cdot\hat{\boldsymbol{\mu}}$ couples the field associated with the photon mode to the molecular dipole operator.[64] The second term, $\hat{H}_{\mathrm{cav}}$, represents the Hamiltonian for the bare cavity mode, which is a harmonic oscillator with fundamental frequency ω. We may also write this in terms of the canonical position and momentum operators for the cavity photon,[65]

$$\hat{H}_{\mathrm{cav}} = \frac{1}{2}\hat{p}^2 + \frac{1}{2}\omega^2\hat{q}^2, \tag{2}$$

where (in atomic units)

$$\hat{p} = i\sqrt{\frac{\omega}{2}}\left(\hat{b}^\dagger - \hat{b}\right), \tag{3}$$

$$\hat{q} = \sqrt{\frac{1}{2\omega}}\left(\hat{b}^\dagger + \hat{b}\right). \tag{4}$$

Next, we apply the coherent state transformation to Eq. (1), which has been done, e.g., in QED-Hartree–Fock, QED-CC, QED-CIS, and QED-CASCI,[28,29,36,41] yielding the Pauli–Fierz Hamiltonian in the coherent state basis,

$$\hat{H}_{\mathrm{CS}} = \hat{H}_e + \hat{H}_{\mathrm{cav}} - \sqrt{\frac{\omega}{2}}[\hat{d} - \langle\hat{d}\rangle_0](\hat{b}^\dagger + \hat{b}) + \frac{1}{2}[\hat{d} - \langle\hat{d}\rangle_0]^2. \tag{5}$$

This follows from a unitary transformation of the Pauli–Fierz Hamiltonian,

$$\hat{H}_{\mathrm{CS}} = \hat{U}_{\mathrm{CS}}\hat{H}_{\mathrm{PF}}\hat{U}_{\mathrm{CS}}^\dagger, \tag{6}$$

where the unitary coherent state transformation is defined as

$$\hat{U}_{\mathrm{CS}} = \exp\left(z(\hat{b}^\dagger - \hat{b})\right), \tag{7}$$

where the parameter z may be computed as

$$z = -\frac{\langle\hat{d}\rangle_0}{\sqrt{2\omega}}. \tag{8}$$

The expectation value $\langle\hat{d}\rangle_0$ will depend on the choice of electronic state. Often, the Hartree–Fock (or QED-HF) reference state is used

to compute this expectation value, but there are other valid choices. We will discuss in a Sec. II B how the coherent state transformation can be seen as shift operator to the photonic position operator, although we can also see the impact of the transformation directly on the photonic ladder operators as follows:

$$\hat{U}_{\mathrm{CS}}\hat{b}\hat{U}_{\mathrm{CS}}^{\dagger} = \hat{b} - z, \tag{9}$$

$$\hat{U}_{\mathrm{CS}}\hat{b}^{\dagger}\hat{U}_{\mathrm{CS}}^{\dagger} = \hat{b}^{\dagger} - z. \tag{10}$$

Although we will refer to the terms $-\sqrt{\frac{\omega}{2}}[\hat{d} - \langle\hat{d}\rangle](\hat{b}^{\dagger} + \hat{b})$ and $\frac{1}{2}[\hat{d} - \langle\hat{d}\rangle_0]^2$ in Eq. (5) as the bilinear coupling and dipole self-energy terms in the coherent state Hamiltonian, respectively, we note that the coherent state transformation does not render these terms fully equivalent to their counterparts in the Pauli–Fierz Hamiltonian. With this caveat in mind, we will endeavor to elucidate the properties of the coherent state transformation that can accelerate the convergence of ai-QED approaches by specifically examining the behavior of the Eqs. (1) and (5) projected onto a subspace of many-electron states that arise from full configuration interaction (FCI) calculations, which is also called a parameterized QED approach (pQED).[18,40,44] In our analysis of these projected Hamiltonians, we will take $\langle\hat{d}\rangle_0$ from the ground state wavefunction from a FCI calculation of the molecule without coupling to the cavity.

A. Perturbation theory for the coupled ground state

We will perform perturbation theory on the Pauli–Fierz Hamiltonian and on the coherent state Hamiltonian, Eq. (1) or (5), projected onto a truncated basis of adiabatic electronic states. For additional details and discussion of the details of this projection and its use in ai-QED methods, see Refs. 18, 40, 44, and 61. The projected molecular electronic Hamiltonian has the form (for both the Pauli–Fierz and coherent-state Hamiltonians)

$$\mathcal{H}_{\mathrm{e}} = \sum_{\alpha} E_{\alpha}|\psi_{\alpha}\rangle\langle\psi_{\alpha}|, \tag{11}$$

where E_α and $|\psi_\alpha\rangle$ are the energy eigenvalues of the adiabatic eigenstates, respectively. In this work, we will obtain these energies and eigenstates from FCI calculations outside of the cavity, and we will denote the projected Hamiltonian operators with calligraphic font as in Eq. (11). The bilinear coupling terms has the form

$$\mathcal{H}_{\mathrm{PF,blc}} = -\sqrt{\frac{\omega}{2}}\sum_{\alpha\beta} d_{\alpha\beta}|\psi_{\alpha}\rangle\langle\psi_{\beta}|\left(\hat{b}^{\dagger} + \hat{b}\right) \tag{12}$$

for the Pauli–Fierz Hamiltonian and upon coherent state transformation, takes the form

$$\mathcal{H}_{\mathrm{CS,blc}} = -\sqrt{\frac{\omega}{2}}\left(\hat{b}^{\dagger} + \hat{b}\right)\left(\sum_{\alpha\beta} d_{\alpha\beta}|\psi_{\alpha}\rangle\langle\psi_{\beta}| - \langle\hat{d}\rangle_0\sum_{\alpha}|\psi_{\alpha}\rangle\langle\psi_{\alpha}|\right), \tag{13}$$

where $d_{\alpha\beta} = \langle\psi_\alpha|\hat{d}|\psi_\beta\rangle$ results from dotting the coupling vector into the transition dipole moment between adiabatic states α and β or the total dipole moment of state α when $\alpha = \beta$. Finally, the dipole self-energy has the form

$$\mathcal{H}_{\mathrm{PF,dse}} = \frac{1}{2}\sum_{\alpha\beta\gamma} d_{\alpha\gamma}d_{\gamma\beta}|\psi_{\alpha}\rangle\langle\psi_{\beta}| \tag{14}$$

for the Pauli–Fierz Hamiltonian and

$$\mathcal{H}_{\mathrm{CS,dse}} = \frac{1}{2}\left[\sum_{\alpha\beta} d_{\alpha\beta}|\psi_{\alpha}\rangle\langle\psi_{\beta}| - \langle\hat{d}\rangle_0\sum_{\alpha}|\psi_{\alpha}\rangle\langle\psi_{\alpha}|\right]^2 \tag{15}$$

for the coherent state Hamiltonian.

If we identify our zeroth-order Hamiltonian as

$$\mathcal{H}_0 = \mathcal{H}_{\mathrm{e}} + \mathcal{H}_{\mathrm{cav}}, \tag{16}$$

we can see that the product states of the adiabatic states $|\psi_\alpha\rangle$ and photon number states $|m\rangle$ are appropriate zeroth-order states satisfying

$$\mathcal{H}_0|\psi_N^{(0)}\rangle = E_N^{(0)}|\psi_N^{(0)}\rangle, \tag{17}$$

with $|\psi_N^{(0)}\rangle = |\psi_{\mu_N}\rangle \otimes |m_N\rangle$ and $E_N^{(0)} = E_{\mu_N} + m_N(\omega + \frac{1}{2})$. In this notation, we are using Greek letters subscripted by upper-case Roman letters (e.g. μ_N) to label the electronic contribution to the zeroth-order product state N and lower-case Roman letters subscripted by upper-case Roman letters (e.g. m_N) to label the photonic contribution to the zeroth-order product state N. It follows then that the perturbation can be regarded as

$$\mathcal{H}' = \mathcal{H}_{\mathrm{blc}} + \mathcal{H}_{\mathrm{dse}}, \tag{18}$$

so that we can write the total the perturbative expansion of the Pauli–Fierz or coherent state Hamiltonian as

$$\mathcal{H} = \mathcal{H}_0 + \epsilon\mathcal{H}'. \tag{19}$$

Using this partitioning, we can derive perturbative energy corrections with and without application of the coherent state transformation and compare these corrections for the same coupling parameters.

The first-order energy correction for the Pauli–Fierz Hamiltonian is

$$E_{\mathrm{N,PF}}^{(1)} = \langle\psi_N^{(0)}|\mathcal{H}'|\psi_N^{(0)}\rangle = \langle\psi_N^{(0)}|\mathcal{H}_{\mathrm{PF,dse}}|\psi_N^{(0)}\rangle = \frac{1}{2}\sum_{\gamma} d_{\mu_N\gamma}d_{\gamma\mu_N}, \tag{20}$$

and the first-order energy correction for the coherent state Hamiltonian is

$$\begin{aligned} E_{\mathrm{N,CS}}^{(1)} &= \langle\psi_N^{(0)}|\mathcal{H}'|\psi_N^{(0)}\rangle = \langle\psi_N^{(0)}|\mathcal{H}_{\mathrm{CS,dse}}|\psi_N^{(0)}\rangle \\ &= \frac{1}{2}\sum_{\gamma} d_{\mu_N\gamma}d_{\gamma\mu_N} - \langle\hat{d}\rangle_0 d_{\mu_N\mu_N} + \frac{1}{2}\langle\hat{d}\rangle_0^2. \end{aligned} \tag{21}$$

The bilinear coupling term does not contribute to the first-order correction since the bra and ket have the same photon occupation state.

The second-order correction to Pauli–Fierz energy is given as

$$\begin{aligned} E^{(2)}_{\mathrm{N,PF}} &= \sum_{M\neq N} \frac{|\langle \psi^{(0)}_M | \mathcal{H}' | \psi^{(0)}_N \rangle|^2}{E^{(0)}_N - E^{(0)}_M} \\ &= \sum_{M\neq N} \frac{|\langle \psi^{(0)}_M | \mathcal{H}_{\mathrm{PF,blc}} | \psi^{(0)}_N \rangle|^2}{E^{(0)}_N - E^{(0)}_M} + \frac{|\langle \psi^{(0)}_M | \mathcal{H}_{\mathrm{PF,dse}} | \psi^{(0)}_N \rangle|^2}{E^{(0)}_N - E^{(0)}_M} \\ &= \frac{\omega}{2}\sum_{\mu_M} \frac{|d_{\mu_M\mu_N}\sqrt{m_N+1}|^2}{E_{\mu_N} - E_{\mu_M} - \omega\hbar} + \frac{\omega}{2}\sum_{\mu_M} \frac{|d_{\mu_M\mu_N}\sqrt{m_N}|^2}{E_{\mu_N} - E_{\mu_M} + \omega\hbar} \\ &\quad + \frac{1}{4}\sum_{\mu_M\neq\mu_N} \frac{|\sum_\gamma d_{\mu_M\gamma} d_{\gamma\mu_N}|^2}{E_{\mu_N} - E_{\mu_M}}. \end{aligned} \tag{22}$$

In this case, both the bilinear coupling and the dipole self-energy terms contribute to the second-order energy correction, but we note that the second line of Eq. (22) does not contain cross terms between the dipole self-energy and the bilinear coupling because the former can only contribute when the bra and the ket have the same photon occupation number, and the latter only contributes when the bra and ket differ by one photon occupation number. Similarly, for the second-order correction to the coherent state energy contains both bilinear coupling and dipole self-energy terms, and the cross terms between them vanish as well. Here, we will first expand out these contributions separately as

$$\begin{aligned} E^{(2)}_{\mathrm{N,CS\ blc}} &= \sum_{M\neq N} \frac{|\langle \psi^{(0)}_M | \mathcal{H}_{\mathrm{CS,blc}} | \psi^{(0)}_N \rangle|^2}{E^{(0)}_N - E^{(0)}_M} \\ &= \frac{\omega}{2}\sum_{\mu_M} \frac{\left|\left(d_{\mu_M\mu_N} - \langle \hat{d} \rangle_0 \delta_{\mu_M\mu_N}\right)\sqrt{m_N+1}\right|^2}{E_{\mu_N} - E_{\mu_M} - \omega\hbar} \\ &\quad + \frac{\omega}{2}\sum_{\mu_M} \frac{\left|\left(d_{\mu_M\mu_N} - \langle \hat{d} \rangle_0 \delta_{\mu_M\mu_N}\right)\sqrt{m_N}\right|^2}{E_{\mu_N} - E_{\mu_M} + \omega\hbar} \end{aligned} \tag{23}$$

for the bilinear coupling and

$$\begin{aligned} E^{(2)}_{\mathrm{N,CS\ dse}} &= \sum_{M\neq N} \frac{|\langle \psi^{(0)}_M | \mathcal{H}_{\mathrm{CS,\,dse}} | \psi^{(0)}_N \rangle|^2}{E^{(0)}_N - E^{(0)}_M} \\ &= \frac{1}{4}\sum_{\mu_N\neq\mu_N} \frac{\left|\sum_\gamma d_{\mu_M\gamma} d_{\gamma\mu_N} - \langle \hat{d} \rangle_0 d_{\mu_M\mu_N}\right|^2}{E_{\mu_N} - E_{\mu_M}} \end{aligned} \tag{24}$$

for the dipole self-energy.

The third-order corrections can be written generically as

$$\begin{aligned} E^{(3)}_{\mathrm{N}} &= \sum_{P,Q\neq N} \frac{\langle \psi^{(0)}_N | \mathcal{H}' | \psi^{(0)}_P \rangle \langle \psi^{(0)}_P | \mathcal{H}' | \psi^{(0)}_Q \rangle \langle \psi^{(0)}_Q | \mathcal{H}' | \psi^{(0)}_N \rangle}{(E^{(0)}_N - E^{(0)}_P)(E^{(0)}_N - E^{(0)}_Q)} \\ &\quad - \langle \psi^{(0)}_N | \mathcal{H}' | \psi^{(0)}_N \rangle \sum_{M\neq N} \frac{|\langle \psi^{(0)}_M | \mathcal{H}' | \psi^{(0)}_N \rangle|^2}{(E^{(0)}_N - E^{(0)}_M)^2}. \end{aligned} \tag{25}$$

We provide more detailed expressions for the third-order corrections, as well as ways to factorize the evaluation of these terms, in the supplementary material. We can see in the above-mentioned expressions that the coherent state transformation introduces offsets to the matrix elements that arise in the perturbative corrections, particularly along the diagonal elements of these corrections. A general trend is that each additional *even* valued correction provides coupling to one additional photonic Fock state. For example, the second-order correction provides coupling between photonic number states $|0\rangle$ and $|1\rangle$, and the fourth-order correction provides coupling between $|0\rangle$, $|1\rangle$, and $|2\rangle$, and so on. Further details are provided in the supplementary material.

B. Perturbation theory for cavity photon

We can take a slightly different perspective than given in Sec. II A and consider the matter subsystem to provide a perturbation on the cavity mode. Here, we will define the zeroth-order Hamiltonian as only the bare cavity Hamiltonian and will consider the perturbation as arising strictly through the bilinear coupling. This will provide insight into the convergence of the photonic subspace in practical coupled calculations. We neglect the dipole self-energy term in this discussion because the dipole self-energy does not contain photonic operators, it only contains matter operators.

The bare cavity Hamiltonian can be written as

$$\hat{H}_{0,\mathrm{cav}} = \frac{1}{2}\hat{p}^2 + \frac{1}{2}\omega^2\hat{q}^2 = \hbar\omega\left(\hat{b}^\dagger\hat{b} + \frac{1}{2}\right), \tag{26}$$

where $\hat{p}$ and $\hat{q}$ were defined in Eq. (3). Recalling the definitions of $\hat{d} = \boldsymbol{\lambda}\cdot\hat{\boldsymbol{\mu}}$, where $\boldsymbol{\lambda} = \sqrt{\frac{1}{\epsilon_0 V}}\hat{\mathbf{e}}$, we can express the bilinear coupling as

$$\hat{H}_{\mathrm{blc}} = -\sqrt{\frac{\omega}{2}}\hat{d}\left(\hat{b}^\dagger + \hat{b}\right) = -\omega\hat{d}\hat{q}. \tag{27}$$

We can now take the point of view that the matter perturbs the cavity Hamiltonian through the bilinear coupling term. In this point of view, the bare cavity Hamiltonian can be used as the zeroth-order Hamiltonian satisfying the eigenvalue equation,

$$\hat{H}_{0,\mathrm{cav}}|n^{(0)}\rangle = E^{(0)}_n|n^{(0)}\rangle = \hbar\omega\left(n + \frac{1}{2}\right)|n^{(0)}\rangle, \tag{28}$$

and the bilinear coupling term can be the perturbation. The perturbed Hamiltonian for the cavity mode interacting with a polarized matter subsystem can then be written as

$$\begin{aligned} \hat{H}_{\mathrm{cav}} &= \hat{H}_{0,\mathrm{cav}} + \hat{H}_{\mathrm{blc}}, \\ \hat{H}_{\mathrm{cav}} &= \frac{1}{2}\hat{p}^2 + \frac{1}{2}\omega^2\hat{q}^2 - \omega\hat{d}\hat{q}, \\ \hat{H}_{\mathrm{cav}} &= \frac{1}{2}\hat{p}^2 + \frac{1}{2}\left(\omega\hat{q} - \hat{d}\right)^2 - \frac{1}{2}\hat{d}^2, \\ \hat{H}_{\mathrm{cav}} &= \hbar\omega\left(\hat{b}^\dagger\hat{b} + \frac{1}{2}\right) - \sqrt{\frac{\omega}{2}}\hat{d}\left(\hat{b}^\dagger + \hat{b}\right). \end{aligned} \tag{29}$$

The perturbation contains a product of $\hat{d}$ and $\hat{q}$, where the former is a matter operator and the latter a photon operator. The exact eigenstates of this Hamiltonian will self-consistently balance the impact of the photon field on the charges in the matter subsystem and the polarization of the photon field by the charges in the matter subsystem. If, however, we replace the operator $\hat{d}$ with an expectation value

$\langle \hat{d} \rangle$ representing the average polarization of the charges in the matter subsystem subject to the photon field, an intuitive picture arises for the photon field subject to an effective potential that arises from the polarized matter. Here, we can look specifically at the third line of Eq. (29) and integrate over the electronic degrees of freedom,

$$\hat{H}_{\text{cav}} = \frac{1}{2}\hat{p}^2 + \frac{1}{2}\left(\omega\hat{q} - \langle \hat{d} \rangle\right)^2 - \frac{1}{2}\langle \hat{d} \rangle^2, \tag{30}$$

where $\langle \hat{d} \rangle$ in an expectation value in terms of an exact electronic eigenstate of the coupled system, which of course is not typically known *a priori*. We can see that this is simply the original cavity Hamiltonian displaced from equilibrium by $\langle \hat{d} \rangle$ and with the total energy shifted by the constant $-\frac{1}{2}\langle \hat{d} \rangle^2$. This shifted Hamiltonian will have the same spectrum of eigenstates as the original Hamiltonian save for a constant shift of all eigenvalues by $-\frac{1}{2}\langle \hat{d} \rangle^2$.

Here, we will use perturbative analysis to elucidate how the coherent state transformation can accelerate the convergence of practical calculations of the eigenstates of the Pauli–Fierz Hamiltonian, where one generally takes as the basis the photon number states that are eigenstates of the zeroth-order Hamiltonian. Although the shapes of these zeroth-order states match those of the eigenstates of the perturbed Hamiltonian, it will require an expansion of a number of these zeroth-order functions to reproduce the perturbed eigenstates, and this number will increase with the magnitude of the displacement of the potential that goes as $\langle \hat{d} \rangle$.

In particular, let us consider the first- and second-order correction to photonic state $|n\rangle$,

$$\begin{aligned} |n^{(1)}\rangle &= -\sum_{m\neq n} \frac{\langle m^{(0)}|\omega\langle \hat{d} \rangle \hat{q}|n^{(0)}\rangle}{E_n^{(0)} - E_m^{(0)}} |m^{(0)}\rangle, \\ |n^{(2)}\rangle &= \sum_{k\neq n}\sum_{n\neq n} \frac{\langle k^{(0)}|\omega\langle \hat{d} \rangle \hat{q}|m^{(0)}\rangle\langle m^{(0)}|\omega\langle \hat{d} \rangle \hat{q}|n^{(0)}\rangle}{(E_n^{(0)} - E_m^{(0)})(E_n^{(0)} - E_k^{(0)})} |k^{(0)}\rangle. \end{aligned} \tag{31}$$

We note that the position operator $\hat{q}$ can only couple adjacent zeroth-order states, that is, only $\langle n^{(0)}|\hat{q}|(n\pm 1)^{(0)}\rangle$ are non-zero. However, we have a contribution to the first-order correction to state $|n\rangle$ that scales linearly with $\omega\langle \hat{d} \rangle$ and couples to states adjacent to $|n\rangle$. The second-order correction scales quadratically with $\omega\langle \hat{d} \rangle$ and brings in coupling to states with $|(n\pm 1)\rangle$ and $|(n\pm 2)\rangle$. This trend will continue to higher orders of correction to the states and is illustrative that for large values of $\omega\langle \hat{d} \rangle$, it will become very difficult to practically converge calculations using the zeroth-order photon basis. This echoes the numerical findings of DePrince III and co-workers[36] and Vu *et al.*[41] who found that large numbers of photon number states were required to converge variational calculations for polar molecules with strong coupling and for charged molecules under displacements from the origin, both circumstances where $\langle \hat{d} \rangle$ can become large. We will see that application of the coherent state transformation can, at least in certain cases, diminish the magnitude of the couplings that necessitate these corrections. We have also observed that the coherent state transformation can render ai-QED methods manifestly origin invariant for charged molecules, and we can examine these perturbative corrections to examine how this arises.

We can view the coherent state transformation as applying shift to the position coordinate as follows:

$$\hat{U}_{\text{CS}}\,\hat{q}\,\hat{U}_{\text{CS}}^{\dagger} = \hat{q} + \frac{\langle \hat{d} \rangle_0}{\omega}, \tag{32}$$

so that we can view the coherent state transformed Hamiltonian for the cavity coupled to polarized matter as

$$\hat{U}_{\text{CS}}\hat{H}_{\text{cav}}\hat{U}_{\text{CS}}^{\dagger} = \frac{1}{2}\hat{p}^2 + \frac{1}{2}\left(\omega\hat{q} + \langle \hat{d} \rangle_0 - \hat{d}\right)^2 - \frac{1}{2}\hat{d}^2. \tag{33}$$

If we again average over the electronic degrees of freedom in the coherent state transformed cavity Hamiltonian, then Eq. (34) becomes

$$\hat{U}_{\text{CS}}\hat{H}_{\text{cav}}\hat{U}_{\text{CS}}^{\dagger} \approx \frac{1}{2}\hat{p}^2 + \frac{1}{2}\left(\omega\hat{q} + \langle \hat{d} \rangle_0 - \langle \hat{d} \rangle\right)^2 - \frac{1}{2}\langle \hat{d} \rangle^2, \tag{34}$$

which un-shifts the potential to within the difference between the expectation value of $\langle \hat{d} \rangle_0$ evaluated with a specific reference function and the exact expectation values $\langle \hat{d} \rangle$, which we will denote $\delta_{\langle d \rangle} = \langle \hat{d} \rangle - \langle \hat{d} \rangle_0$. Inserting the same relationship into the perturbative correction to the states yields

$$\begin{aligned} |n^{(1)}\rangle &= -\sum_{m\neq n} \frac{\langle m^{(0)}|\omega\delta_{\langle d \rangle} \hat{q}|n^{(0)}\rangle}{E_n^{(0)} - E_m^{(0)}} |m^{(0)}\rangle, \\ |n^{(2)}\rangle &= \sum_{k\neq n}\sum_{m\neq n} \frac{\langle k^{(0)}|\omega\delta_{\langle d \rangle} \hat{q}|m^{(0)}\rangle\langle m^{(0)}|\omega\delta_{\langle d \rangle} \hat{q}|n^{(0)}\rangle}{(E_n^{(0)} - E_m^{(0)})(E_n^{(0)} - E_k^{(0)})} |k^{(0)}\rangle. \end{aligned} \tag{35}$$

Thus, while the perturbative corrections in Eq. (31) scale as orders of $\omega\langle \hat{d} \rangle$, the corrections in Eq. (35) scale as orders of $\omega\delta_{\langle \hat{d} \rangle}$, which will tend to be small as long as the cavity coupling does not lead to changes to the molecular dipole moment that are larger than the uncoupled dipole moment itself.

To see how the coherent state transformation imparts origin invariance, recall that $\hat{d}$ is defined as the lambda vector dotted into the dipole, $\hat{d} = \lambda \cdot \hat{\mu}$, where the dipole operator $\hat{\mu} = \sum_i z_i r_i$, so we can rewrite $\hat{d} = \lambda \cdot \sum_i z_i r_i$. The expectation value is then defined as $\langle \hat{d} \rangle = \lambda \cdot \sum_i z_i \langle \psi | r_i | \psi \rangle$, where ψ is the electronic contribution to the target eigenstate, which is unaffected by the coherent state transformation since $\hat{U}_{\text{CS}}$ acts only on photonic coordinates. While $\hat{d}$ itself is not origin invariant if the molecule has net charge, $\delta_{\langle d \rangle}$ is origin invariant. To see this, we will consider the expectation value $\langle \hat{d}' \rangle$ following displacement by Δr,

$$\langle \hat{d}' \rangle = \lambda \cdot \left(\sum_i z_i (\langle \psi | r_i | \psi \rangle + \Delta r) \right) = \langle \hat{d} \rangle + \lambda \cdot \Delta r \sum_i z_i, \tag{36}$$

which shows that $\langle \hat{d} \rangle$ is itself origin-dependent. Similarly, we will write $\langle \hat{d}' \rangle_0$ following displacement by the same Δr as

$$\langle \hat{d}' \rangle_0 = \lambda \cdot \left(\sum_i z_i (\langle \Phi_0 | r_i | \Phi_0 \rangle + \Delta r) \right) = \langle \hat{d} \rangle_0 + \lambda \cdot \Delta r \sum_i z_i, \tag{37}$$

so that we see $\langle \hat{d} \rangle_0$ has the same origin dependence. Finally, we consider $\delta_{\langle d' \rangle}$,

$$\delta_{\langle d' \rangle} = \langle \hat{d} \rangle + \lambda \cdot \Delta r \sum_i z_i - \langle \hat{d} \rangle_0 - \lambda \cdot \Delta r \sum_i z_i = \langle \hat{d} \rangle - \langle \hat{d} \rangle_0, \quad (38)$$

which is origin invariant.

III. COMPUTATIONAL DETAILS

We formulate perturbative corrections to Pauli–Fierz and coherent state transformed Hamiltonians projected onto a subspace of adiabatic many-electron states and photonic Fock states. The adiabatic many-electron states are computed using full configuration interaction (FCI) using the qed-ci package,[66] which interfaces with the psi4 package for standard electron integrals.[67,68] We take variational calculations of the projected Pauli–Fierz Hamiltonian in a sufficiently large basis of electronic and photonic states (herein referred to as variational pQED) to be the numerically exact answer and compare the perturbative corrections to this variational calculation in all cases. All the variational and perturbative calculations are also performed using the qed-ci package. We apply these approaches to the helium hydride cation (HeH^+), lithium hydride (LiH), and hydroxide anion (OH^-). We represent the HeH^+ system in the cc-pVQZ[69] (the results from cc-pVDZ and cc-pVTZ are shown in the supplementary material), and we represent LiH in a 6-311G basis set[70] and OH^- in a 6-31G basis set. For all variational calculations, we consider a photonic Fock space with ten number states ($|0\rangle, |1\rangle, \ldots, |9\rangle$); these details are summarized in Table I. A glossary of acronyms used in describing the various perturbative and variational approaches is presented in Table II.

A. Physical meaning of coupling strengths

We consider a range of coupling strengths quantified by the magnitude of the fundamental coupling vector $\boldsymbol{\lambda}$ ranging between 0.001 and 0.1 a.u. We can relate the magnitude of this coupling vector to the cavity volume using the relation $\lambda = \sqrt{\frac{1}{\epsilon V}} = \sqrt{\frac{4\pi}{V}}$, where $\frac{1}{\epsilon_0} = 4\pi$ in atomic units. The smallest coupling magnitude of 0.001 a.u. corresponds to a cavity volume of ~1860 nm^3, and the largest coupling strength of 0.1 a.u. corresponds to a cavity volume of ~0.186 nm^3. These ranges are specifically explored for the helium hydride cation system. For the lithium hydride and hydroxide cation, we report results with the magnitude of the coupling strength fixed at 0.05 a.u., which corresponds to a cavity volume of ~0.75 nm^3.

We can also relate the coupling to an energy scale and compare that to the resonance or cavity energies in each case, where the energy corresponding to a given coupling strength can be determined as $E_{\text{coupling}} = \sqrt{\frac{\omega}{2}}\boldsymbol{\lambda} \cdot \boldsymbol{\mu}$. For the helium hydride system, we are coupling specifically through the $S_0 \rightarrow S_2$ transition that has a transition dipole moment along the z axis of 0.8 a.u. Given that the transition energy is 26 eV, the range of coupling energies is between 0.015 and 1.5 eV. This puts the relative coupling energy roughly between 0.06% and 6% of the transition energy for the helium hydride cation system. For the lithium hydride system, we are coupling the $S_0 \rightarrow S_1$ transition with a transition dipole moment of roughly 1 a.u. with a transition energy of 3.28 eV, so the coupling energy is roughly 0.33 eV, or about 10% of the transition energy. For the hydroxide anion, we do not couple to any specific transition, but we find the permanent dipole moment is roughly 0.18 a.u. and the photon energy is 5.96 eV, so the coupling energy is 0.08 eV or about 1.4% of the photon energy. For all systems, this could be considered strong coupling, provided the cavity dissipation energy scale is less than roughly 3.75 meV (this condition is generally considered to be reached when the coupling energy scale exceeds one fourth of the dissipation energy scale), but not ultra-strong coupling, which requires the coupling energy scale to be on the order of 50% of the transition energy.[17,18]

TABLE I. Summary of the orbital basis, size of the adiabatic many-electron basis, and (for variational calculations) size of the photonic Fock state basis for calculations presented in the results section.

System	Orbital basis	N_{el}	N_p
HHe^+	cc-pVQZ	2880	10
LiH	6–311g	500	10
OH^-	6-31G	50	10

IV. RESULTS

We provide several illustrative numerical examples of the behavior of the coherent state transformation following the discussion in Secs. II A and II B. In particular, to illustrate the discussion in Sec. II A, we will consider the second- and third-order perturbative corrections to the ground state energy of the helium hydride ion

TABLE II. Glossary of acronyms used to describe different methodologies used in this work.

pQED(N_{el}, N_p)	Variational solution of Eq. (1) projected onto a basis of N_{el} adiabatic many electron states and N_p photonic Fock states
PF-PT2(N_{el})	Second-order perturbative approximation to Eq. (1) projected onto a basis of N_{el} adiabatic many electron states
PF-PT3(N_{el})	Third-order perturbative approximation to Eq. (1) projected onto a basis of N_{el} adiabatic many electron states
CS-PT2(N_{el})	Second-order perturbative approximation to Eq. (5) projected onto a basis of N_{el} adiabatic many electron states
CS-PT3(N_{el})	Third-order perturbative approximation to Eq. (5) projected onto a basis of N_{el} adiabatic many electron states

and the lithium hydride molecule. In both cases, we will compare the resulting ground state estimates to the variational result that we obtain after projecting the Pauli–Fierz Hamiltonian onto a very large subspace of electronic states and photonic states, which we will take to be the exact ground state of the projected Pauli–Fierz Hamiltonian. The orbital, many-electron, and photonic Fock basis details for each system are provided in Sec. III A.

A. Peturbation theory for the coupled ground state

1. Helium hydride cation

We first consider the HeH^+ cation coupled to a cavity mode resonant with the first dipole allowed transition ($S_0 \rightarrow S_2$), which has a transition dipole moment oriented along the inter-nuclear axis (the z axis shown in Fig. 1). We fix the geometry at the equilibrium bond length found at the (cavity free) FCI/cc-pVTZ level, which is 0.77 Å. At this geometry, the ground state has a permanent dipole moment of 1.73 Debye along the z axis, and the $S_0 \rightarrow S_2$ transition energy has an energy of 26.1 eV. We fix the energy of the cavity mode to be on resonance with this transition and consider values λ_z ranging from 0 to 0.1 a.u. Although these coupling conditions can lead to the formation of polariton states, in this work, we focus exclusively on the ground state of the coupled system. Degenerate perturbation theory is required to resolve the degeneracies that will arise when polariton states are targeted and will be the subject of future work.

The behavior of the ground-state energies to second- and third-order of perturbation theory to Eq. (1) (PF-PT2(2880)/cc-pVQZ and PF-PT3(2880)/cc-pVQZ) and Eq. (5) (CS-PT2(2880)/cc-pVQZ and CS-PT3(2880)/cc-pVQZ) are shown in Figs. 2 and 3, with errors reported relative to the exact variational ground state computed at the pQED(2880,10)/cc-pVQZ level. In the top panel of Fig. 2, we have $E_g(\lambda) - E_g(0)$ plotted vs coupling strength, where $E_g(\lambda)$ is the energy of the coupled system with λ representing the coupling strength, and $E_g(0)$ is the energy of the uncoupled system. This plot shows the exact $E_g(\lambda) - E_g(0)$ from pQED(2880,10)/cc-pVQZ and the CS and PF formulations of second-order perturbation theory. The energy of the system increases as coupling between the molecule and the cavity increases; thus, the size of the perturbation also increases. We observe that both the PT2

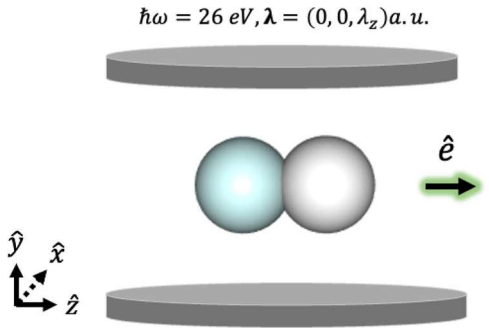

FIG. 1. Schematic of HeH^+ coupled to a cavity mode polarized along the inter-nuclear axis (z) and tuned to the first optically allowed transition from $S_0 \rightarrow S_2$ at ~26 eV.

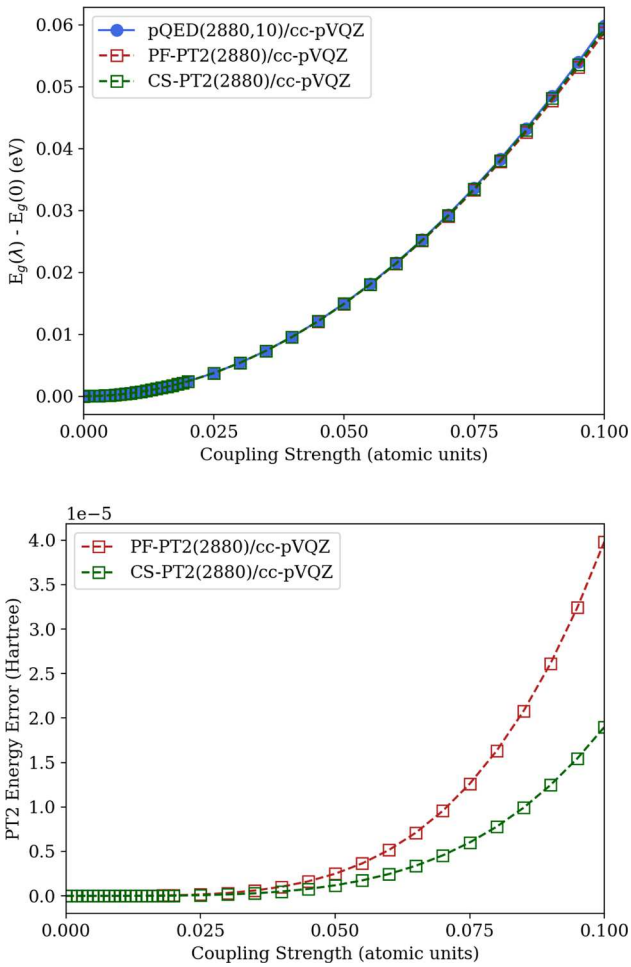

FIG. 2. Ground state energy from second-order perturbation theory for HeH^+ coupled to a cavity photon with $\hbar\omega = 26$ eV across a range of coupling strengths. (Top) Relative energy of the coupled ground state as a function of coupling strength as computed by a fully converged variational approach to the Pauli–Fierz Hamiltonian and by second-order perturbation theory for the Pauli–Fierz and coherent state Hamiltonians. (Bottom) Error of second-order perturbation theory for the PF and CS Hamiltonians relative to the fully converged variational calculation as a function of coupling strength.

results have negligible error when the coupling strength is less than $\lambda_z \approx 0.025$ a.u., but starts to depart for stronger coupling (see Fig. 2, bottom panel). At the larger values of λ_z, CS-PT2 has a consistently smaller error compared to PF-PT2. The top panel of Fig. 3 is similar to Fig. 2 except the former now has the third-order perturbative approximations to pQED. Again, we see that the CS-PT3 and PF-PT3 energies have negligible error for small coupling strength and again start to depart for values of lambda larger than $\lambda_z \approx 0.025$ a.u., and again, CS-PT3 has consistently smaller errors than the PF-PT3 results (see Fig. 3, bottom panel).

2. Lithium hydride bond stretch

The LiH ground state potential energy surface is computed between bond lengths of 1.4 and 2.2 Å coupled to a cavity mode

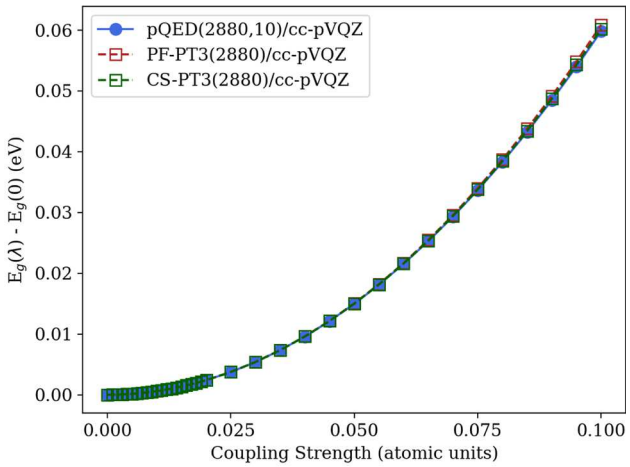

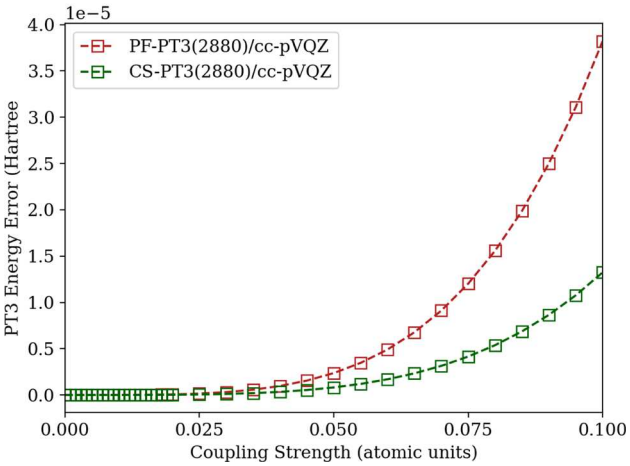

FIG. 3. Ground state energy from second-order perturbation theory for HeH^+ coupled to a cavity photon with $\hbar\omega$ = 26 eV across a range of coupling strengths. (Top) Relative energy of the coupled ground state as a function of coupling strength as computed by a fully converged variational approach to the Pauli–Fierz Hamiltonian and by third-order perturbation theory for the Pauli–Fierz and coherent state Hamiltonians. (Bottom) Error of third-order perturbation theory for the PF and CS Hamiltonians relative to the fully converged variational calculation as a function of coupling strength.

with frequency $\hbar\omega_{cav}$ = 3.28 eV polarized along the z axis with λ_z = 0.05 a.u. (see Fig. 4). We compare PF-PT2(500)/6-311G and CS-PT2(500)/6-311G to exact variational potential energy surface [pQED(500,10)/6-311G] shown in Fig. 5, and the PT3 analogs are compared to the exact variational potential energy surface shown in Fig. 6.

As with the HHe+ system, the CS-PT2 and CS-PT3 results are consistently closer to the numerically exact pQED results compared to the PF-PT2 and PF-PT3 results. It can be seen in Fig. 5 that the CS-PT2 and PF-PT2 curves are both lower bounds to the exact variational curve, with the CS-PT2 being closer across the stretch. Furthermore, we see in Fig. 6 that the CS-PT3 and PF-PT3 curves are upper bounds to the exact curve, with the CS-PT3 being closer to

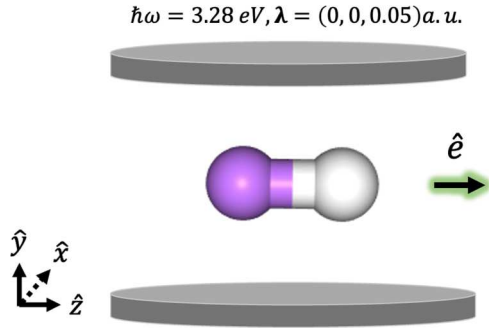

FIG. 4. Schematic of the LiH coupled to a cavity mode polarized along the internuclear axis (z) and tuned to the first optically allowed transition from $S_0 \rightarrow S_1$ at ~3.28 eV.

the variational curve across the stretch. In Table III, the root mean squared (RMS) error between the perturbative approaches and the pQED across the bond length scan are presented. Interestingly, we see the CS-PT2 result has the smallest RMS error. While the CS-PT3 RMS error is smaller than the PF-PT3 RMS error, we observe that the PF-PT3 RMS error is slightly larger than the PF-PT2 error just as the CS-PT3 RMS error is slightly larger than the CS-PT2 RMS error.

Plots of magnitude and relative errors for the perturbative approaches vs pQED(500,10)/6-311G are shown in the supplementary material for λ_z values of 0.01 and 0.05 shown in Figs. S5 and S6, respectively. The trajectories of the errors shown in Figs. S5 and S6 show a systematic increase with increasing bond length, suggesting that the magnitude of the light–matter coupling

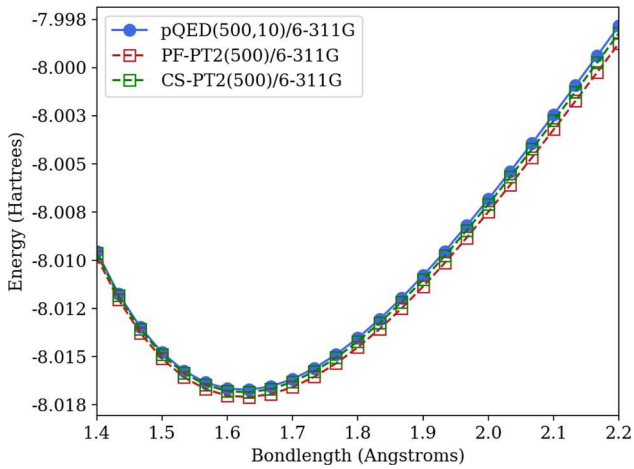

FIG. 5. Ground state potential energy surface for LiH coupled to a cavity photon with $\hbar\omega$ = 3.28 eV across a range of r values with a coupling strength of 0.05 a.u. Relative energy of the coupled ground state as a function of bond length computed by using a fully converged variational approach to the Pauli–Fierz Hamiltonian and by second-order perturbation theory for the Pauli–Fierz and coherent state Hamiltonians.

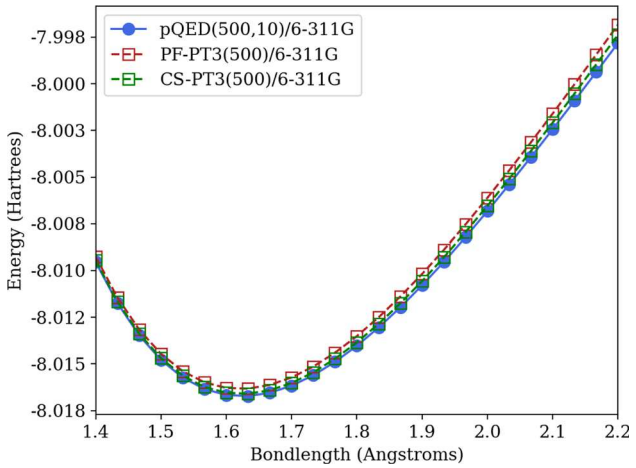

FIG. 6. Ground state potential energy surface for LiH coupled to a cavity photon with $\hbar\omega$ = 3.28 eV across a range of r values with a coupling strength of 0.05 au. Relative energy of the coupled ground state as a function of bond length computed by using a fully converged variational approach to the Pauli–Fierz Hamiltonian and by third-order perturbation theory for the Pauli–Fierz and coherent state Hamiltonians.

TABLE III. Comparison of mean squared errors for different levels of theory for the LiH PES under strong coupling. The errors are calculated with respect to pQED(500,10).

Level of theory	Root mean squared error (hartrees)
PF-PT2(500)	5.58×10^{-4}
PF-PT3(500)	5.97×10^{-4}
CS-PT2(500)	2.18×10^{-4}
CS-PT3(500)	2.36×10^{-4}

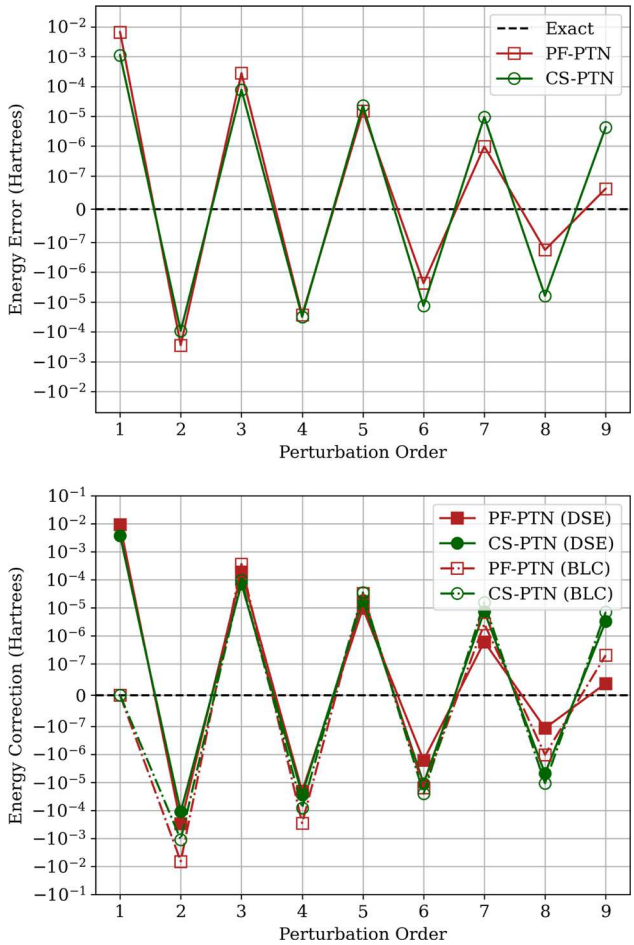

FIG. 7. Perturbative corrections for LiH coupled to a cavity photon with $\hbar\omega$ = 3.28 eV with r fixed at 1.4 Å and with a coupling strength of 0.05 au. The error of the perturbative energy at a given order for both PF and CS Hamiltonians is plotted relative to the exact ground state energy from the pQED(500,10)/6-311G level.

increases similarly. This is likely attributable to the monotonic increases in the magnitude of the dipole moment as the LiH bond is stretched (see Fig. S7). An important requirement for the validity of perturbation theory is that the magnitude of the perturbation is relatively small, and failure of this criterion leads to non-convergent perturbative series where subsequent orders of perturbation theory take one further away, rather than closer, to the exact answer. To investigate if these results are evidence of a non-convergent perturbative series, we apply perturbation theory up to ninth order with and without the coherent state transformation for the same LiH system at the shortest bond length (1.4 Å) with coupling strength λ_z = 0.05 a.u. In the top panel of Fig. 7, we show the energy error relative to the exact pQED(500,10)/6-311G energy at each order for PF-PTN and CS-PTN up to N = 9, showing that both series are systematically converging to the exact answer. In the bottom panel of Fig. 7, we partition the N^{th} order energy correction into bilinear coupling (BLC) and dipole self-energy (DSE) terms for both the Pauli–Fierz and coherent state Hamiltonians. Additional details on computing arbitrary orders of perturbation theory and partitioning the corrections into bilinear coupling and dipole self-energy terms are given in Eqs. (S24) and (S25) in the supplementary material. We see that in the progression of energy errors, the error of (both PF and CS) PT2 and PT3 are quite similar in magnitude, that the errors of PT4 and PT5 are similar and have decreased by about an order of magnitude relative to PT2 and PT3, and that the errors associated with PT6 and PT7 are similar and have decreased relative to PT4 and PT5. Thus, we see in this system that PT3 does not provide a substantial reduction in error over PT2, but PT4 does. This finding is similar to what is found in many chemical contexts using Møller–Plesset perturbation theory.[71] What is particularly interesting to see for this case is that for correction orders 1 through 3, the coherent state transformation clearly performs better than the same corrections to the Pauli–Fierz Hamiltonian, but the perturbative series for the Pauli–Fierz Hamiltonian converges more rapidly, and so by orders ≥ 6, the Pauli–Fierz Hamiltonian clearly performs better (and both approaches behave similarly for orders 4 and 5, see Fig. 7, top panel). We hypothesize that the reason for the better performance of lower orders of CS-PTN is that at these

lower orders, the advantages of photonic Fock space convergence afforded by the coherent state transformation are more significant, whereas for larger perturbative orders, the errors associated with photonic Fock space truncation in PF-PTN are negligible for the coupling conditions considered in this work. To see the impact of photonic Fock space truncation, we can look at the convergence behavior of full diagonalization of the Pauli–Fierz and coherent state Hamiltonians under different levels of Fock space truncation with a saturated basis of adiabatic electronic states, shown graphically in Fig. S8. We find that for the LiH system, four photonic Fock states are required to converge the Pauli–Fierz ground state energy to sub-microhartree errors; three photonic Fock states are required to converge the ground state energy of the coherent state Hamiltonian to sub-microhartree error (see Fig. S8). The coupling between up to four photonic Fock states will be included in the ground state correction afforded at the PF-PN6 level, and so we should expect that errors arising from truncated coupling between photonic Fock states becomes negligible for orders greater than or equal to six. Alternatively, PF-PN2 and PF-PN3 for the ground state only permit coupling between two photonic Fock states and PF-PN4 and PF-PN5 will enable coupling between three photonic Fock states. The truncation error from full diagonalization of the Pauli–Fierz Hamiltonian projected onto two photonic Fock states is associated with an error of roughly a half a millihartree, as shown in Fig. S8, and the truncation to three Fock states is associated with an error of tens of microhartrees [see Fig. S8 and Eqs. (S3)–(S7) for analysis of the third-order terms in terms of photonic Fock state coupling, and see Eqs. (S21)–(S23) for the same analysis of orders four through six].

B. Perturbation theory for the cavity ground state

To further elucidate the impact of the coherent state transformation on the convergence of the photonic subspace, we consider two examples of the matter subsystem perturbing the cavity Hamiltonian. In the first example, we revisit the lithium hydride system as an example of a polar molecule that can strongly perturb the cavity Hamiltonian through bilinear coupling, and we illustrate how the coherent state transformation can effectively mitigate this perturbation. In the second example, we consider the hydroxide anion as a charged species that has an origin-dependent dipole moment. This property of charged species can induce very large perturbations to cavity modes when the molecule is displaced away from the cavity origin, and in the un-transformed representation, can impart a strong origin dependence in the energy that necessitates a large photonic Fock spaces to numerically resolve.

1. Lithium hydride

We again consider the LiH molecule within the 6-311G basis set with a bond length of 1.55 Å coupled to a photon with frequency $\hbar\omega_{\mathrm{cav}} = 3.28$ eV (0.1208 hartrees) polarized along the z axis with $\lambda_z = 0.2$ a.u. We choose a large value of λ to clearly illustrate the impact of strong coupling on the cavity potential, and the bond length of 1.55 Å was chosen as the equilibrium bond length for these cavity conditions. In the top panel of Fig. 8, we illustrate the bare cavity potential given by $V(\hat{q}) = \frac{1}{2}\omega_{\mathrm{cav}}^2\hat{q}^2$ indicated by the solid black lines and the perturbed potential given by

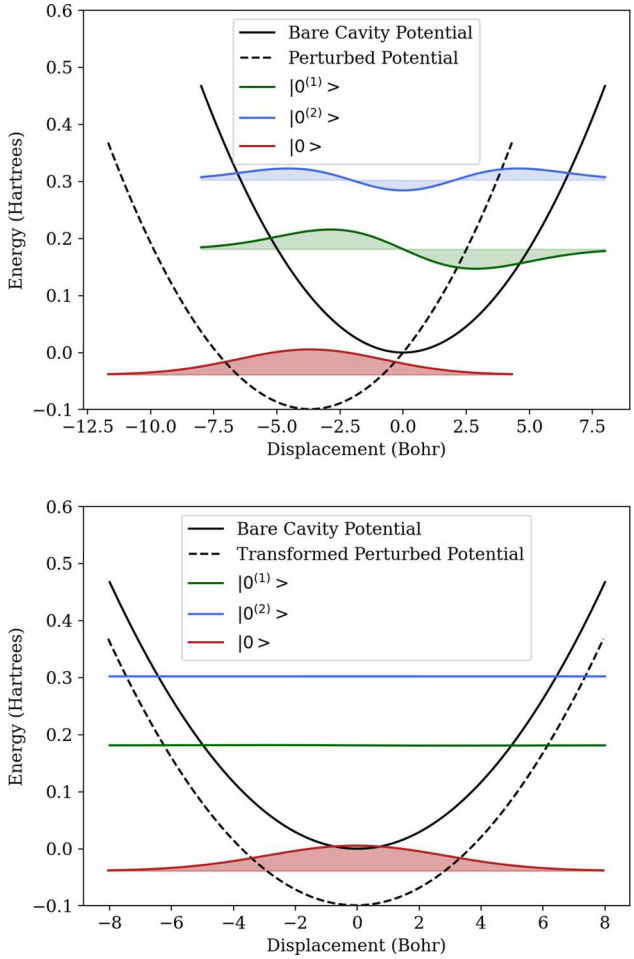

FIG. 8. Top panel: illustration of the polarization of a cavity mode with $\omega_{\mathrm{cav}} = 3.28$ eV through bilinear coupling to the LiH molecule with coupling strength $\lambda_z = 0.2$ a.u. The unperturbed (solid black) and perturbed (dashed black) potentials are plotted along with the exact ground-state wavefunction for the cavity mode on the perturbed potential, and its first- and second-order corrections on the unperturbed potential. Bottom panel: the same system is represented following application of the coherent state transformation to the cavity Hamiltonian.

$V'(\hat{q}) = \frac{1}{2}\omega_{\mathrm{cav}}^2\hat{q}^2 - \omega_{\mathrm{cav}}\langle\hat{d}\rangle\hat{q}$ indicated by the dashed black lines. The large displacement of these potentials is indicative of the magnitude of the cavity polarization imparted by the bilinear coupling to the polar matter subsystem. The expectation value $\langle\hat{d}\rangle$ is computed at the pQED(500,10)/6-311G level and $\langle\hat{d}\rangle_0$ is computed at the FCI/6-311G level (see Sec. III A for more details). We plot the exact ground-state cavity wavefunction for the perturbed system $|0\rangle$ on the perturbed potential (see Fig. 8, top panel). Due to the polarization induced by the bilinear coupling, the $|0\rangle$ state has considerable coupling to excited zeroth-order states ($|n^{(0)}\rangle$ with $n > 0$). We capture this coupling through the first- and second-order corrections to state $|0\rangle$ in the top panel of Fig. 8, where the contributions $|0^{(1)}\rangle$ and $|0^{(2)}\rangle$ are shown on the unperturbed potential. In particular, these corrections have the explicit form

$$|0^{(1)}\rangle = \frac{\langle \hat{d} \rangle}{\sqrt{2}\omega_{\text{cav}}}|1^{(0)}\rangle,$$
$$|0^{(2)}\rangle = \frac{\langle \hat{d} \rangle^2}{2\sqrt{2}\omega_{\text{cav}}}|2^{(0)}\rangle, \tag{39}$$

where we have evaluated Eq. (31) analytically to obtain these expressions in terms of $\langle \hat{d} \rangle$ and ω_{cav}. Numerical values for the first- and second-order coefficients are presented in Table IV, and we can visually see that there is considerable contribution from the first- and second-order corrections owing to the magnitude of the bilinear coupling term. The bottom panel of Fig. 8 shows the perturbed potential following coherent state transformation, $\hat{U}_{\text{CS}} V'(\hat{q}) \hat{U}_{\text{CS}}^{\dagger} = \frac{1}{2}(\omega_{\text{cav}}\hat{q} + \langle \hat{d} \rangle_0 - \langle \hat{d} \rangle)^2 - \frac{1}{2}\langle \hat{d} \rangle)^2$, in a dashed black line against the unperturbed potential in solid black line, and again, we plot the exact state $|0\rangle$ along the transformed perturbed potential and the first- and second-order corrections ($|0^{(1)}\rangle$ and $|0^{(2)}\rangle$) along the unperturbed potential. We can clearly see the impact of the transformation on the location of the minima of the potential, which is now visibly indiscernible from the minima of the unperturbed potential. Similarly, we can see that the first- and second-order corrections to state $|0\rangle$ are vanishingly small following the transformation (see Fig. 8, bottom panel). The first- and second-order coefficients can again be evaluated analytically by substituting $\delta_{\langle d \rangle}$ for $\langle \hat{d} \rangle$ in Eq. (39), and are tabulated in Table IV, where we see the first-order coefficient is roughly 75 times smaller in magnitude the second-order coefficient is more than 5000 times smaller in magnitude following the coherent state transformation. This illustrates how the coherent state transformation can effectively mitigate the polarization of the cavity models by polar matter that would typically necessitate a large number of photonic Fock states to recover.

2. Hydroxide anion

To illustrate the ability of coherent state transformation to ensure numerical origin invariance for energies of charged molecules, we consider the hydroxide anion displaced 20 Å from the cavity origin (see Fig. 9). We wish to emphasize that in the long wavelength limit assumed by the Pauli–Fierz and coherent state Hamiltonians, the vector potential and electric field associated with the cavity mode does not have spatial variation, so the energy of the coupled system should not depend on the placement of the molecule relative to the cavity origin. Nevertheless, truncation of the photonic subspace in finding the eigenstates of the Pauli–Fierz Hamiltonian for charged systems can lead to origin-dependent energies as has been discussed in several instances in the literature.[36,37] We attempt to elucidate this numerical difficulty through the subsequent results and discussion.

TABLE IV. Coefficients for first- and second-order corrections to the ground state cavity wavefunction for the LiH and displaced OH^- system with and without coherent state transformation.

	Without transformation		With transformation	
System	$c^{(1)}$	$c^{(2)}$	$c^{(1)}$	$c^{(2)}$
LiH	-9.06×10^{-1}	5.80×10^{-1}	-1.24×10^{-2}	1.08×10^{-4}
OH^-	-2.80×10^{0}	5.57×10^{0}	5.11×10^{-4}	1.85×10^{-7}

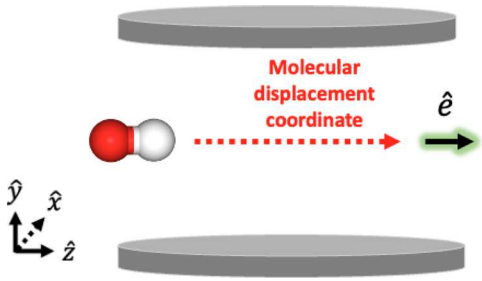

FIG. 9. Schematic of OH^- displaced from the cavity origin. The cavity mode has energy of $\hbar\omega = 5.96$ eV with $\lambda_z = 0.05$ a.u., polarized along the internuclear axis of the molecule.

The OH^- anion is represented within the 6-31G basis set with a bond length of 0.9 Å coupled to a photon with frequency $\hbar\omega_{\text{cav}} = 5.96$ eV (0.219 hartrees) polarized along the z axis with $\lambda_z = 0.05$ a.u. We note that this field does not couple directly to a transition in the molecule; while there is a dipole allowed transition at 5.96 eV, in this coordinate system, it does not have a transition dipole moment along the polarization axis of the field. Therefore, the coupling occurs through the permanent dipole moment of the molecule. The expectation value $\langle \hat{d} \rangle$ is computed at the pQED(50,10)/6-31G level, and $\langle \hat{d} \rangle_0$ is computed at the FCI/6-31G level. The top panel of Fig. 10 shows the unperturbed cavity potential (solid black line), the perturbed potential when the molecule is at the cavity origin (dashed–dotted black line), and the perturbed potential when the molecule is displaced by 20 Å from the cavity origin (dashed black line). We can see the profound influence that the origin-dependent dipole moments have on the displacement of the perturbed potential. While the perturbed potential from the molecule at the cavity origin is almost indiscernible from the unperturbed potential at this coupling strength, the perturbed potential from the displaced molecule is dramatically displaced. In other words, the hydroxide anion provides some intrinsic polarization of the cavity state and also has a polarizing effect that is proportional to its displacement from the cavity origin owing to its origin-dependent dipole moment. For this particular system (i.e. the cavity coupling strength and the displacement), the polarization arising from the molecular displacement is much more dramatic. We also see that this polarization imparts even stronger coupling between the ground state wavefunction of the perturbed cavity and excited zeroth-order states (see the top panel of Fig. 10). However, application of the coherent state transformation completely eliminates the polarization that arises from displacement from the cavity origin and (similar to what was demonstrated for LiH) results in cavity polarization that is proportional to $\delta_{\langle \hat{d} \rangle}$. Accordingly, we see that the transformed potential aligns closely with the unperturbed potential, and the coupling between the cavity ground state and excited zeroth-order states is almost entirely eliminated (see the bottom panel of Fig. 10). In this case, we see even more dramatic reduction in the magnitude of the first- and second-order coefficients following coherent state transformation: the first-order coefficient is more than 5000 times smaller in magnitude and the second-order coefficient is more than

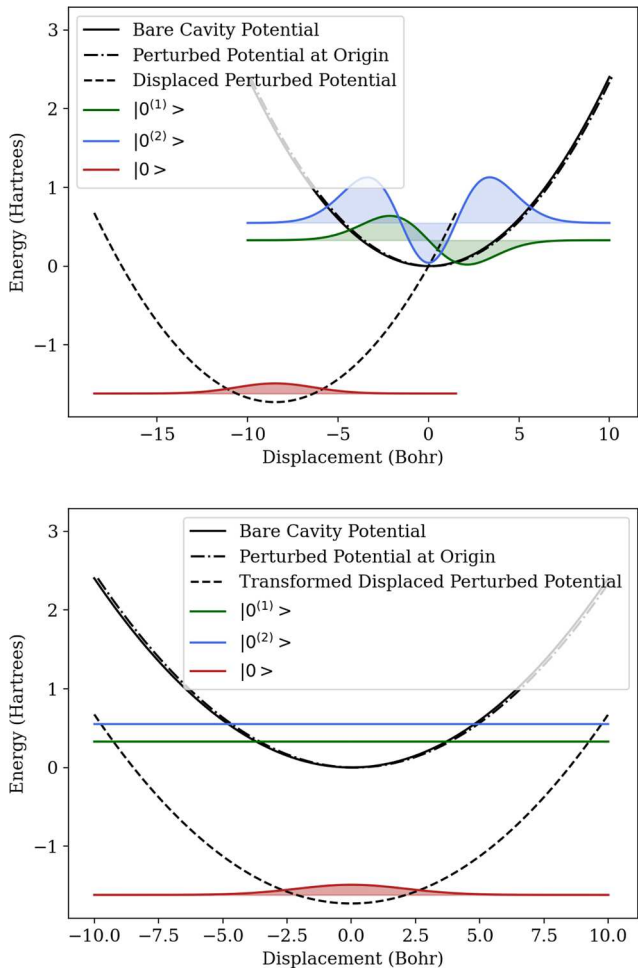

FIG. 10. Top panel: illustration of the polarization of a cavity mode with ω_{cav} = 5.96 eV through bilinear coupling to the OH^- anion with coupling strength λ_z = 0.05 a.u. with and without displacement of the anion from the cavity origin. The unperturbed (solid black) and perturbed potentials that arise when the molecule shares the same origin as the cavity (dashed–dotted black) and when it is displaced from the cavity origin (dashed black) are plotted along with the exact ground-state wavefunction for the cavity mode on the perturbed potential, and its first- and second-order corrections on the unperturbed potential. Bottom panel: the same system is represented following application of the coherent state transformation to the cavity Hamiltonian.

seven orders of magnitude times smaller following the coherent state transformation.

V. CONCLUDING REMARKS

In this work, we utilized perturbation theory to elucidate favorable computational properties, namely, faster convergence of the photonic Fock space and robustly origin-invariant energies, which arise when coherent state transformation is applied to *ab initio* QED methodologies. In particular, we found that applying the coherent state transformation yields second- and third-order estimates to the ground state energy that are in consistently better agreement with exact ground state across a range of coupling strengths compared to the same orders without transformation of the Hamiltonian. We applied arbitrary order perturbation theory for one test system with the largest relative coupling energy scale to confirm that the perturbative series for both the Pauli–Fierz Hamiltonian and its coherent state transformed analog converged to the exact answer. This analysis showed that, for this system, the advantage of the coherent state transformation was only a feature of low orders of correction and that perturbative corrections of order 6 and higher to the Pauli–Fierz Hamiltonian gave better agreement with the exact ground state. We hypothesized that this behavior is consistent with the coherent state transformation primarily enhancing the convergence with respect to the photonic subspace and that perturbative orders of 6 and higher to the Pauli–Fierz Hamiltonian effectively saturate the photonic Fock space under these coupling conditions and for the ground state. It remains an open question if this behavior persists into the ultra-strong coupling regime or if it applies to polariton states where degenerate perturbation theory would be required. Consistent with our hypothesis about photonic Fock space convergence, when we treated the bilinear coupling between electron and photon degrees of freedom as a perturbation to the cavity Hamiltonian, we found that the coherent state transformation decouples the systems to within a magnitude that is related to the error in the reference estimate of the dipole moment expectation value that parameterizes the transformation for a target coupled state. We showed that this error is manifestly origin invariant, and so this result sheds light on why the coherent state transformation accelerates photon convergence and restores origin invariance in *ab initio* QED calculations.

SUPPLEMENTARY MATERIAL

The supplementary material contains detailed third order corrections to the ground state, including factorized expressions for efficient computational evaluation; analysis of fourth-, fifth-, and sixth-order energy corrections in terms of photonic Fock state coupling; key equations for arbitrary order perturbation theory; and additional supporting figures illustrating the behavior of different perturbative corrections to the systems provided in the main text, as well as the photonic Fock space truncation error for the lithium hydride system.

ACKNOWLEDGMENTS

J.J.F. and P.R. gratefully acknowledge the financial support from NSF CAREER Award No. CHE-2043215. J.J.F. acknowledges UNC Charlotte for startup funds.

AUTHOR DECLARATIONS

Conflict of Interest

The authors have no conflicts to disclose.

Author Contributions

Peyton Roden: Formal analysis (equal); Investigation (equal); Software (equal); Writing – original draft (equal); Writing – review &

editing (equal). **Jonathan J. Foley IV**: Conceptualization (equal); Formal analysis (equal); Funding acquisition (equal); Project administration (equal); Supervision (equal); Validation (equal); Writing – original draft (equal); Writing – review & editing (equal).

DATA AVAILABILITY

Open-source implementation of the methods used for the results presented within can be accessed in the following GitHub repository: https://github.com/mapol-chem/qed-ci/tree/jcp_submission.

The data that support the findings of this study are available from the corresponding author upon reasonable request; json data corresponding to the results in Sec. IV A may be found https://github.com/FoleyLab/data_repository/; specifically for HeH^+ data here: https://github.com/FoleyLab/data_repository/tree/main/Mapol/HHep/perturbation_theory and for LiH data here: https://github.com/FoleyLab/data_repository/tree/main/Mapol/LiH/perturbation_theory. An example Jupyter notebook producing the figures and coefficients used in results Sec. IV B may be found here: https://github.com/FoleyLab/SCQED-PCQED/blob/perturbation_theory/src/OHminus_PT_for_Cavity.ipynb.

REFERENCES

[1] A. Frisk Kockum, A. Miranowicz, S. De Liberato, S. Savasta, and F. Nori, "Ultrastrong coupling between light and matter," Nat. Rev. Phys. **1**, 19–40 (2019).
[2] J. Flick, N. Rivera, and P. Narang, "Strong light-matter coupling in quantum chemistry and quantum photonics," Nanophotonics **7**, 1479–1501 (2018).
[3] P. Törmä and W. L. Barnes, "Strong coupling between surface plasmon polaritons and emitters: A review," Rep. Prog. Phys. **78**, 013901 (2014).
[4] D. G. Lidzey, D. D. C. Bradley, M. S. Skolnick, T. Virgili, S. Walker, and D. M. Whittaker, "Strong exciton–photon coupling in an organic semiconductor microcavity," Nature **395**, 53–55 (1998).
[5] J. Bellessa, C. Bonnand, J. C. Plenet, and J. Mugnier, "Strong coupling between surface plasmons and excitons in an organic semiconductor," Phys. Rev. Lett. **93**, 036404 (2004).
[6] J. A. Hutchison, T. Schwartz, C. Genet, E. Devaux, and T. W. Ebbesen, "Modifying chemical landscapes by coupling to vacuum fields," Angew. Chem., Int. Ed. **51**, 1592–1596 (2012).
[7] D. M. Coles, Y. Yang, Y. Wang, R. T. Grant, R. A. Taylor, S. K. Saikin, A. Aspuru-Guzik, D. G. Lidzey, J. K.-H. Tang, and J. M. Smith, "Strong coupling between chlorosomes of photosynthetic bacteria and a confined optical cavity mode," Nat. Commun. **5**, 5561 (2014).
[8] E. Orgiu, J. George, J. A. Hutchison, E. Devaux, J. F. Dayen, B. Doudin, F. Stellacci, C. Genet, J. Schachenmayer, C. Genes, G. Pupillo, P. Samorì, and T. W. Ebbesen, "Conductivity in organic semiconductors hybridized with the vacuum field," Nat. Mater. **14**, 1123–1129 (2015).
[9] R. Chikkaraddy, B. de Nijs, F. Benz, S. J. Barrow, O. A. Scherman, E. Rosta, A. Demetriadou, P. Fox, O. Hess, and J. J. Baumberg, "Single-molecule strong coupling at room temperature in plasmonic nanocavities," Nature **535**, 127–130 (2016).
[10] T. W. Ebbesen, "Hybrid light–matter states in a molecular and material science perspective," Acc. Chem. Res. **49**, 2403–2412 (2016).
[11] M. Sukharev and A. Nitzan, "Optics of exciton-plasmon nanomaterials," J. Phys.: Condens. Matter **29**, 443003 (2017).
[12] X. Zhong, T. Chervy, L. Zhang, A. Thomas, J. George, C. Genet, J. A. Hutchison, and T. W. Ebbesen, "Energy transfer between spatially separated entangled molecules," Angew. Chem., Int. Ed. **56**, 9034–9038 (2017).
[13] K. Chevrier, J. M. Benoit, C. Symonds, S. K. Saikin, J. Yuen-Zhou, and J. Bellessa, "Anisotropy and controllable band structure in suprawavelength polaritonic metasurfaces," Phys. Rev. Lett. **122**, 173902 (2019).
[14] S. Kéna-Cohen and S. R. Forrest, "Room-temperature polariton lasing in an organic single-crystal microcavity," Nat. Photonics **4**, 371–375 (2010).
[15] N. M. Hoffmann, L. Lacombe, A. Rubio, and N. T. Maitra, "Effect of many modes on self-polarization and photochemical suppression in cavities," J. Chem. Phys. **153**, 104103 (2020).
[16] A. Mandal and P. Huo, "Investigating new reactivities enabled by polariton photochemistry," J. Phys. Chem. Lett. **10**, 5519–5529 (2019).
[17] P. Antoniou, F. Suchanek, J. F. Varner, and J. J. Foley, "Role of cavity losses on nonadiabatic couplings and dynamics in polaritonic chemistry," J. Phys. Chem. Lett. **11**, 9063–9069 (2020).
[18] A. Mandal, M. Taylor, B. Weight, E. Koessler, X. Li, and P. Huo, "Theoretical advances in polariton chemistry and molecular cavity quantum electrodynamics," Chem. Rev. **123**, 9786–9879 (2023).
[19] J. Fregoni, F. J. Garcia-Vidal, and J. Feist, "Theoretical challenges in polaritonic chemistry," ACS Photonics **9**, 1096–1107 (2022).
[20] A. D. Wright, J. C. Nelson, and M. L. Weichman, "Rovibrational polaritons in gas-phase methane," J. Am. Chem. Soc. **145**, 5982–5987 (2023).
[21] M. Ruggenthaler, F. Mackenroth, and D. Bauer, "Time-dependent Kohn-Sham approach to quantum electrodynamics," Phys. Rev. A **84**, 042107 (2011).
[22] I. V. Tokatly, "Time-dependent density functional theory for many-electron systems interacting with cavity photons," Phys. Rev. Lett. **110**, 233001 (2013).
[23] M. Ruggenthaler, J. Flick, C. Pellegrini, H. Appel, I. V. Tokatly, and A. Rubio, "Quantum-electrodynamical density-functional theory: Bridging quantum optics and electronic-structure theory," Phys. Rev. A **90**, 012508 (2014).
[24] C. Pellegrini, J. Flick, I. V. Tokatly, H. Appel, and A. Rubio, "Optimized effective potential for quantum electrodynamical time-dependent density functional theory," Phys. Rev. Lett. **115**, 093001 (2015).
[25] J. Flick, C. Schäfer, M. Ruggenthaler, H. Appel, and A. Rubio, "Ab initio optimized effective potentials for real molecules in optical cavities: Photon contributions to the molecular ground state," ACS Photonics **5**, 992–1005 (2018).
[26] R. Jestädt, M. Ruggenthaler, M. J. T. Oliveira, A. Rubio, and H. Appel, "Light-matter interactions within the Ehrenfest–Maxwell–Pauli–Kohn–Sham framework: Fundamentals, implementation, and nano-optical applications," Adv. Phys. **68**, 225–333 (2019).
[27] J. Flick and P. Narang, "*Ab initio* polaritonic potential-energy surfaces for excited-state nanophotonics and polaritonic chemistry," J. Chem. Phys. **153**, 094116 (2020).
[28] J. McTague and J. J. Foley IV, "Non-hermitian cavity quantum electrodynamics–configuration interaction singles approach for polaritonic structure with *ab initio* molecular Hamiltonians," J. Chem. Phys. **156**, 154103 (2022).
[29] T. S. Haugland, E. Ronca, E. F. Kjønstad, A. Rubio, and H. Koch, "Coupled cluster theory for molecular polaritons: Changing ground and excited states," Phys. Rev. X **10**, 041043 (2020).
[30] A. E. DePrince III, "Cavity-modulated ionization potentials and electron affinities from quantum electrodynamics coupled-cluster theory," J. Chem. Phys. **154**, 094112 (2021).
[31] U. Mordovina, C. Bungey, H. Appel, P. J. Knowles, A. Rubio, and F. R. Manby, "Polaritonic coupled-cluster theory," Phys. Rev. Res. **2**, 023262 (2020).
[32] J. Yang, Q. Ou, Z. Pei, H. Wang, B. Weng, Z. Shuai, K. Mullen, and Y. Shao, "Quantum-electrodynamical time-dependent density functional theory within Gaussian atomic basis," J. Chem. Phys. **155**, 064107 (2021).
[33] J. Yang, Z. Pei, E. C. Leon, C. Wickizer, B. Weng, Y. Mao, Q. Ou, and Y. Shao, "Cavity quantum-electrodynamical time-dependent density functional theory within Gaussian atomic basis. II. Analytic energy gradient," J. Chem. Phys. **156**, 124104 (2022).
[34] M. L. Vidal, F. R. Manby, and P. J. Knowles, "Polaritonic effects in the vibronic spectrum of molecules in an optical cavity," J. Chem. Phys. **156**, 204119 (2022).
[35] N. Vu, G. M. McLeod, K. Hanson, and A. E. I. DePrince, "Enhanced diastereocontrol via strong light–matter interactions in an optical cavity," J. Phys. Chem. A **126**, 9303–9312 (2022).
[36] J. J. Foley IV, J. McTague, and A. E. DePrince III, "*Ab initio* methods for polariton chemistry," Chem. Phys. Rev. **4**, 041301 (2023).
[37] M. D. Liebenthal, N. Vu, and A. E. DePrince III, "Assessing the effects of orbital relaxation and the coherent-state transformation in quantum electrodynamics

density functional and coupled-cluster theories," J. Phys. Chem. A **127**, 5264–5275 (2023).
[38]M. Bauer and A. Dreuw, "Perturbation theoretical approaches to strong light–matter coupling in ground and excited electronic states for the description of molecular polaritons," J. Chem. Phys. **158**, 124128 (2023).
[39]D. Hu and P. Huo, "Ab initio molecular cavity quantum electrodynamics simulations using machine learning models," J. Chem. Theory Comput. **19**, 2353–2368 (2023).
[40]B. M. Weight, T. D. Krauss, and P. Huo, "Investigating molecular exciton polaritons using ab initio cavity quantum electrodynamics," J. Phys. Chem. Lett. **14**, 5901–5913 (2023).
[41]N. Vu, D. Mejia-Rodriguez, N. P. Bauman, A. Panyala, E. Mutlu, N. Govind, and J. J. Foley IV, "Cavity quantum electrodynamics complete active space configuration interaction theory," J. Chem. Theory Comput. **20**, 1214–1227 (2024).
[42]B. M. Weight, S. Tretiak, and Y. Zhang, "Diffusion quantum Monte Carlo approach to the polaritonic ground state," Phys. Rev. A **109**, 032804 (2024).
[43]Z.-H. Cui, A. Mandal, and D. R. Reichman, "Variational Lang–Firsov approach plus Møller–Plesset perturbation theory with applications to ab initio polariton chemistry," J. Chem. Theory Comput. **20**, 1143 (2024).
[44]B. M. Weight, D. J. Weix, Z. J. Tonzetich, T. D. Krauss, and P. Huo, "Cavity quantum electrodynamics enables para- and ortho-selective electrophilic bromination of nitrobenzene," J. Am. Chem. Soc. **146**, 16184 (2024).
[45]J. D. Weidman, M. S. Dadgar, Z. J. Stewart, B. G. Peyton, I. S. Ulusoy, and A. K. Wilson, "Cavity-modified molecular dipole switching dynamics," J. Chem. Phys. **160**, 094111 (2024).
[46]B. G. Peyton, J. D. Weidman, and A. K. Wilson, "Light-induced electron dynamics of molecules in cavities: Comparison of model Hamiltonians," J. Opt. Soc. Am. B **41**, C74–C81 (2024).
[47]Y. E. Moutaoukal, R. R. Riso, M. Castagnola, and H. Koch, "Toward polaritonic molecular orbitals for large molecular systems," J. Chem. Theory Comput. **20**(20), 8911–8920 (2024).
[48]M. Matoušek, N. Vu, N. Govind, J. J. Foley IV, and L. Veis, "Polaritonic chemistry using the density matrix renormalization group method," J. Chem. Theory Comput. **20**(21), 9424–9434 (2024).
[49]M. D. Liebenthal and A. E. DePrince III, "The orientation dependence of cavity-modified chemistry," J. Chem. Phys. **161**, 064109 (2024).
[50]M. T. Lexander, S. Angelico, E. F. Kjønstad, and H. Koch, "Analytical evaluation of ground state gradients in quantum electrodynamics coupled cluster theory," J. Chem. Theory Comput. **20**(20), 8876–8885 (2024).
[51]L. Monzel and S. Stopkowicz, "Diagrams and symmetry in polaritonic coupled cluster theory," arXiv:2407.00757 [physics.chem-ph] (2024).
[52]J. R. Schrieffer and P. A. Wolff, "Relation between the Anderson and Kondo Hamiltonians," Phys. Rev. **149**, 491–492 (1966).
[53]F. J. Wegner, "Flow equations for Hamiltonians," Nucl. Phys. B, Proc. Suppl. **90**, 141–146 (2000), non-perturbative QCD and hadron phenomenology.
[54]T. Helgaker, P. Jorgensen, and J. Olsen, *Molecular Electronic-Structure Theory* (John Wiley & Sons, 2014).
[55]F. A. Evangelista, "A driven similarity renormalization group approach to quantum many-body problems," J. Chem. Phys. **141**, 054109 (2014).
[56]K. Kowalski and N. P. Bauman, "Fock-space Schrieffer–Wolff transformation: Classically-assisted rank-reduced quantum phase estimation algorithm," Appl. Sci. **13**, 539 (2022).
[57]S. D. Folkestad, E. F. Kjønstad, R. H. Myhre, J. H. Andersen, A. Balbi, S. Coriani, T. Giovannini, L. Goletto, T. S. Haugland, A. Hutcheson, I.-M. Høyvik, T. Moitra, A. C. Paul, M. Scavino, A. S. Skeidsvoll, Å. H. Tveten, and H. Koch, "*et* 1.0: An open source electronic structure program with emphasis on coupled cluster and multilevel methods," J. Chem. Phys. **152**, 184103 (2020).
[58]A. Mandal, S. Montillo Vega, and P. Huo, "Polarized Fock states and the dynamical casimir effect in molecular cavity quantum electrodynamics," J. Phys. Chem. Lett. **11**, 9215–9223 (2020).
[59]R. R. Riso, T. S. Haugland, E. Ronca, and H. Koch, "Molecular orbital theory in cavity QED environments," Nat. Commun. **13**, 1368 (2022).
[60]X. Li and Y. Zhang, "First-principles molecular quantum electrodynamics theory at all coupling strengths," arXiv:2310.18228 [physics.chem-ph] (2023).
[61]R. Manderna, N. Vu, and J. J. Foley IV, "Comparing parameterized and self-consistent approaches to *ab initio* cavity quantum electrodynamics for electronic strong coupling," J. Chem. Phys. **161**(17), 174105 (2024).
[62]H. Spohn, *Dynamics of Charged Particles and Their Radiation Field* (Cambridge University Press, Cambridge, 2004).
[63]A. Szabo and N. S. Ostlund, *Modern Quantum Chemistry: Introduction to Advanced Electronic Structure Theory*, 1st ed. (Dover Publications, Inc., Mineola, 1996).
[64]R. H. Myhre, T. J. A. Wolf, L. Cheng, S. Nandi, S. Coriani, M. Gühr, and H. Koch, "A theoretical and experimental benchmark study of core-excited states in nitrogen," J. Chem. Phys. **148**, 064106 (2018).
[65]N. M. Hoffmann, C. Schäfer, A. Rubio, A. Kelly, and H. Appel, "Capturing vacuum fluctuations and photon correlations in cavity quantum electrodynamics with multitrajectory Ehrenfest dynamics," Phys. Rev. A **99**, 063819 (2019).
[66]N. Vu, J. J. F. IV, and R. Manderna, QED-CI: A program for performing cavity quantum electrodynamics configuration interaction calculations (2023), https://github.com/mapol-chem/qed-ci/tree/main (last accessed July 2024).
[67]D. G. A. Smith, L. A. Burns, A. C. Simmonett, R. M. Parrish, M. C. Schieber, R. Galvelis, P. Kraus, H. Kruse, R. Di Remigio, A. Alenaizan, A. M. James, S. Lehtola, J. P. Misiewicz, M. Scheurer, R. A. Shaw, J. B. Schriber, Y. Xie, Z. L. Glick, D. A. Sirianni, J. S. O'Brien, J. M. Waldrop, A. Kumar, E. G. Hohenstein, B. P. Pritchard, B. R. Brooks, H. F. Schaefer, A. Y. Sokolov, K. Patkowski, A. E. DePrince, U. Bozkaya, R. A. King, F. A. Evangelista, J. M. Turney, T. D. Crawford, and C. D. Sherrill, "Psi4 1.4: Open-source software for high-throughput quantum chemistry," J. Chem. Phys. **152**, 184108 (2020).
[68]D. G. A. Smith, L. A. Burns, D. A. Sirianni, D. R. Nascimento, A. Kumar, A. M. James, J. B. Schriber, T. Zhang, B. Zhang, A. S. Abbott, E. J. Berquist, M. H. Lechner, L. A. Cunha, A. G. Heide, J. M. Waldrop, T. Y. Takeshita, A. Alenaizan, D. Neuhauser, R. A. King, A. C. Simmonett, J. M. Turney, H. F. Schaefer, F. A. Evangelista, A. E. DePrince III, T. D. Crawford, K. Patkowski, and C. D. Sherrill, "Psi4numpy: An interactive quantum chemistry programming environment for reference implementations and rapid development," J. Chem. Theory Comput. **14**, 3504–3511 (2018).
[69]T. H. Dunning, Jr. and H. Thom, "Gaussian basis sets for use in correlated molecular calculations. I. The atoms boron through neon and hydrogen," J. Chem. Phys. **90**, 1007–1023 (1989).
[70]R. Krishnan, J. S. Binkley, R. Seeger, and J. A. Pople, "Self-consistent molecular orbital methods. XX. A basis set for correlated wave functions," J. Chem. Phys. **72**, 650–654 (1980).
[71]D. Cremer, "Møller–Plesset perturbation theory: From small molecule methods to methods for thousands of atoms," Wiley Interdiscip. Rev.: Comput. Mol. Sci. **1**, 509–530 (2011).